

EXPLORATION OF INTERMITTENT INSTABILITIES IN A BOOST CONVERTER SUPPLIED FROM A RECTIFIER

raman GEETHA ^{1*}, govindarajan UMA ¹ and subramanian ARCHANA ¹

¹Department of Electrical Engineering
Power Systems Division

Anna University, Chennai-600 025, India

* geethabhargav@gmail.com / eee.geetha@velammal.edu.in

Abstract

This paper presents the researched phenomenon of nonlinear dynamics exhibited by a current controlled boost converter fed from a rectifier as an alternative to a regulated dc supply. The calculated Floquet multipliers from Fillipov's stability technique matches the simulation and hardware prototype result. Bifurcation analysis performed for different parametric values, shows various behavioral patterns. A detailed analysis of unintentional intrusion of signals caused by electromagnetic interference is also presented.

Index Terms—Chaos, Rectifier, Intermittency, Fillipov's theory

1. Introduction

Power electronic converters, being time varying nonlinear dynamical systems are found to exhibit several periodic steady state responses as well as chaotic responses. The importance of the converters and their reliability are emerging trends of research in power electronic circuitry study. The presence of non-ideal switching devices as a key component in switched mode systems, unintentional coupling of spurious signals and the presence of ripple or harmonic components in the supply may all account for the complex behavior of the system. In this context, chaos in a current controlled dc-dc boost converter has been investigated and evaluated with different analytical methods [1]-[3]. The pathways through which the current controlled boost converter exhibit chaos for different parametric variation have also been reported [4]. Bifurcation and chaos analysis for the current controlled boost converter operating in discontinuous conduction mode have also been reported [5]-[6].

The dc supply for dc-dc or dc-ac converters is usually derived from a diode bridge rectifier. The ripple frequency and variations in ripple amplitude strongly influence the converter dynamics. A careful

consideration of these factors has led to an analysis of the rectifier fed voltage mode controlled buck converter [7]. It has been observed that undesirable voltages or currents present in electrical systems may lead to electromagnetic interference (EMI) and may reach the victim device by electromagnetic conduction or radiation [8]. Improper shielding of the power supplies against the interference of intruding signals, presence of non ideal reactive elements, etc. may also lead to intermittent chaotic operation [9]-[10]. Interference can be in the form of coupling through conducted or radiated paths, which may be present in the power circuit board or at a near proximity [11]. The effect of adding spurious signal in the control voltage of a voltage-mode controlled buck converter and intermittency has been studied extensively [12]. Effects of saw-tooth, triangular and sinusoidal interference signals in control and input voltages of the buck converter have also been studied and analyzed [13]. However, the study on nonlinear dynamics of a rectifier fed current mode controlled boost converter with spurious signals perturbation is seldom reported.

This paper primarily focuses on the nonlinear phenomenon exhibited by a rectifier fed current controlled boost converter, along with intrusion of periodic spurious signals. In section 2, the state equations of the system are explained along with the bifurcation behavior of current controlled boost converter fed from a rectifier with different filter capacitor values. In section 3, analysis is extended for the diode bridge rectifier fed current mode controlled boost converter, considering various ripple percentages in input dc voltage followed by experimental studies. In section 4, mathematical analysis using Fillipov's method is carried out. Section 5, details the intrusion of sinusoidal signal in

reference, with rational and irrational frequency ratios. Finally conclusions are drawn in section 6.

2. System Description and Modeling

The circuit diagram and the power circuit schematic of peak current controlled dc-dc boost converter is shown in Fig.1a and 1b, respectively. The converter is fed from a single phase ac supply through (V_{acrms}) a diode bridge rectifier with C filter. L and C_0 are the reactive elements of the converter. 'S' is the controlled switching device. 'D' is the diode and 'R' is the load resistance. i_L is the inductor current and V_0 is the output voltage. v_{dc} and V_{in} are the rectified and filtered voltages, respectively.

The design parameters are:

Switching frequency $f_s = 25$ kHz, $R = 47 \Omega$, $I_{ref} = 1A$, $L = 500\mu H$, $C_0 = 100 \mu F$, and ac supply voltage to the rectifier is $V_{acrms} = 15V$ [14].

When the switch 'S' is 'ON', $i_L(t)$ increases and reaches the reference current value, and when the switch 'S' is 'OFF' the current ramps down to a minimum value.

The state equations of the system during switch 'ON' and 'OFF' are

$$\dot{X} = A_1 X + B_1 V_{in} \quad S \text{ is ON} \quad (1)$$

$$\dot{X} = A_2 X + B_2 V_{in} \quad S \text{ is OFF}$$

where

$$X = \begin{bmatrix} x_1 & x_2 \end{bmatrix}^T = \begin{bmatrix} i_L & v_o \end{bmatrix}^T \quad (2)$$

'X' indicates the state vector of the system.

A_1, A_2 and B_1, B_2 are the system matrices given by:

$$A_1 = \begin{bmatrix} 0 & 0 \\ 0 & -\frac{1}{RC} \end{bmatrix}, A_2 = \begin{bmatrix} 0 & -\frac{1}{L} \\ \frac{1}{C} & -\frac{1}{RC} \end{bmatrix} \quad (3)$$

$$B_2 = B_1 = \begin{bmatrix} \frac{1}{L} \\ 0 \end{bmatrix} \quad (4)$$

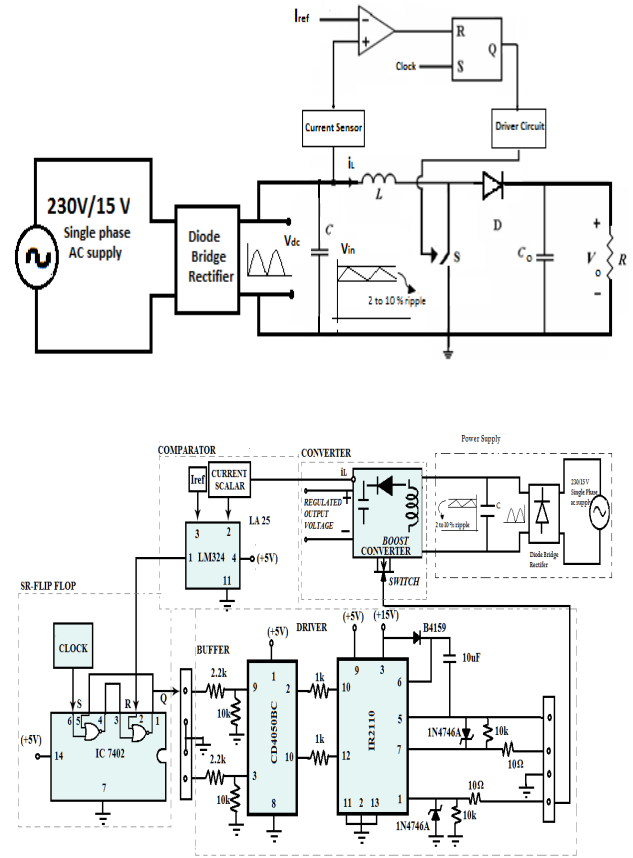


Fig. 1a. Circuit diagram of a peak current controlled boost converter 1b. Hardware realization

3. Analysis of boost converter fed from a diode bridge rectifier

Rectifier is an essential part in power supply unit which is used as an interface between utility and most of the electronic gadgets. Conventionally to obtain dc voltage from an ac source, a diode bridge rectifier is utilized. The filter capacitor used at the rectifier output, limits the ripple peak of the dc input voltage to the converter. In this section, the nonlinear dynamics exhibited by current mode controlled boost converter powered from a single phase rectifier with a filter capacitor is analysed for various input ripple percentages along with variation in system parameters. In a practical scenario, the allowed ripple content [6] in a power supply may vary from 2% to 10%. For a ripple content of 2%, the system becomes bulky and hence 10% ripple content is chosen for analysis. Since the converter is fed from a rectifier with a 50 Hz ac input voltage, the dynamics is governed by the switching frequency of the

converter and the ripple frequency(100 Hz).The rectifier fed current controlled boost converter with bifurcation parameters as I_{ref} , R and V_{in} is simulated and results are discussed below.

3.1 I_{ref} variation

The rectified dc input with 10% ripple is considered for analysis. For I_{ref} variation between 0.5A and 1.3A the system exhibits stable operation. The time plot of inductor current in long span reveals the presence of 100 Hz frequency component and short span plot shows period 1 operation. The Poincare section exhibits a loop like structure showing quasiperiodic [15-16] nature with 250 points instead of a single point due to the presence of commensurable frequencies in the system as shown in Fig. 2(b). When I_{ref} is increased to 1.35A, time plot of inductor current in close span reveals the period 2 nature and the effect of ripple frequency is seen in long span. Further increase in I_{ref} to 1.6A, the system enters the chaotic region. Fig.2 shows the time plot of inductor current (both in long and short span) and corresponding Poincare sections for variation in I_{ref} .

3.2 Capacitance variation

Disturbance in supply voltage is a practical reality and variations in supply voltage makes the system to lose its stability. The dynamics of the current controlled boost converter fed from a stiff dc supply in the presence of intruding signal is analyzed in an extensive manner [9, 10, 12]. This paper considers a widely used rectifier fed boost converter for analysis. To reduce the ripple content of the voltage from the diode bridge rectifier, a capacitor filter is used and to analyze the behavior of peak current mode controlled boost converter different capacitance values are used. The time bifurcation diagram of inductor current for $C=4700\mu F$ is shown in Fig.3 (a) showing a stable operation. Then, the system starts to lose its periodicity at the beginning of each half line cycle, which is depicted in Fig.3(b), for $C=1000\mu F$. When $C=600\mu F$ and $C=120\mu F$ the converter enters into chaotic region via intermittency. From Fig.3, the following conclusions are drawn.

- it can be easily seen a periodic instability exists in each half line cycle.
- reduction in capacitance value reduces the region of stable period one

- ripple current value increases with decrease in C value

3.3 Load Variation

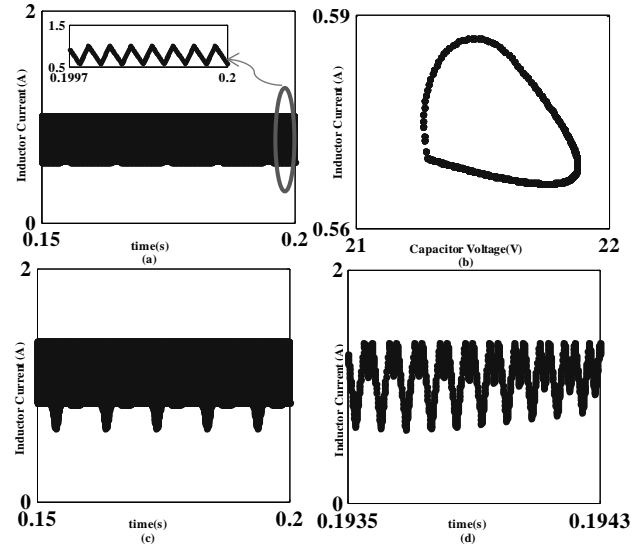


Fig.2 Time Plot of Inductor Current in Long span with I_{ref} (a)1A (c) 1.35 A ;Zoomed version shows the time plot of Inductor Current in short span; (b) Corresponding Poincare section with $I_{ref} = 1$ A ; (d)time plot of Inductor Current in short span $I_{ref} = 1.35$ A

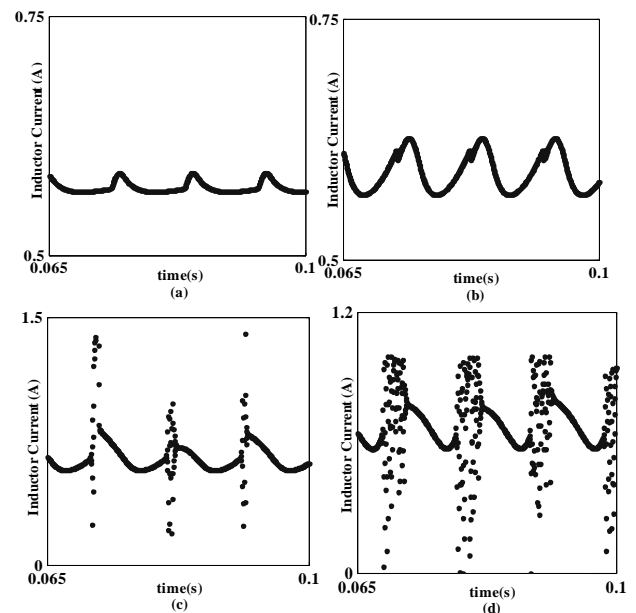


Fig.3 Time Bifurcation diagram of peak current mode controlled boost converter with C variation (a) $4700\mu F$ (b) $1000\mu F$ (c) $600\mu F$ (d) $120\mu F$

3.3 Load Variation

Naturally every system will undergo variation in load. Increase in R makes the system to lose its periodic nature and spikes are observed in time plot of inductor current in long span.

In short span, the variation from period 1 ($R=47\ \Omega$) Fig.2(a) to period 2 ($R=80\ \Omega$) and then to chaotic mode ($R=100\ \Omega$) is clearly visible. Figs. 4(a) and 4(b) represent the period 2 variation in long span and short span clearly. Similarly Figs.4 (c) and 4(d) represent the chaotic behavior with $R=100\ \Omega$.

With R as bifurcation parameter and with a ripple content of 2% in V_{dc} (across C), the system exhibits various behavioural patterns. For $R=47\ \Omega$, the system exhibits stable operation [7].

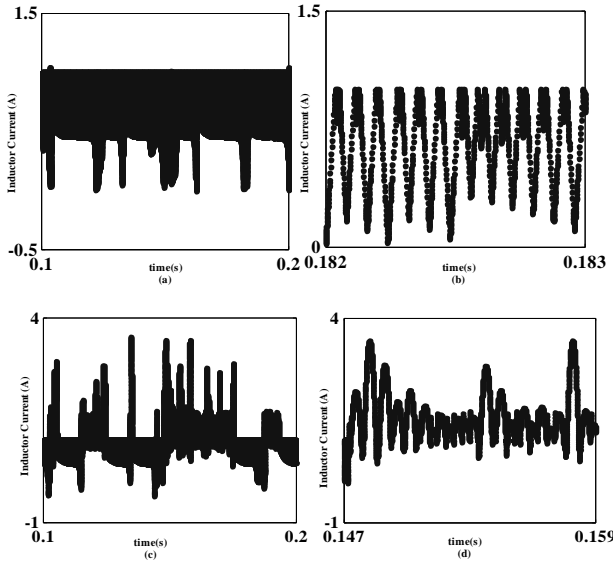


Fig.4 Time response of inductor current waveform (a) $R=80\ \Omega$ (c) $R=100\ \Omega$ in long span and Corresponding short span waveform in (b), (d)

When R is increased to $80\ \Omega$, the discrete state space contains two disjoint mirror image elliptical structures each having 125 points, as shown in Fig.5 (b) revealing the period-2 operation. The time plot of inductor current in long span shown in Fig.5 (a) reveals the presence of ripple frequency (100Hz) and short span reveals the presence of period 2 nature. As R is further increased to $90\ \Omega$, the inner loop in each elliptical curve shrinks as shown in Fig.5 (d) revealing the diminishing effect of 25000 Hz component and system operates in period 2 steady state. Time plot of inductor current waveform

for $R=90\ \Omega$ and $95\ \Omega$ in long span are shown in Fig.5 (c) and Fig 6 (b) respectively. Fig 6 (a) shows the long span waveform for $R=95\ \Omega$ and Fig 6 (b) is the corresponding Poincare section.

With increase in R to $100\ \Omega$ the disjoint mirror structures are distancing themselves from each other and the system enters into DCM, which is shown in Fig.6 (d).

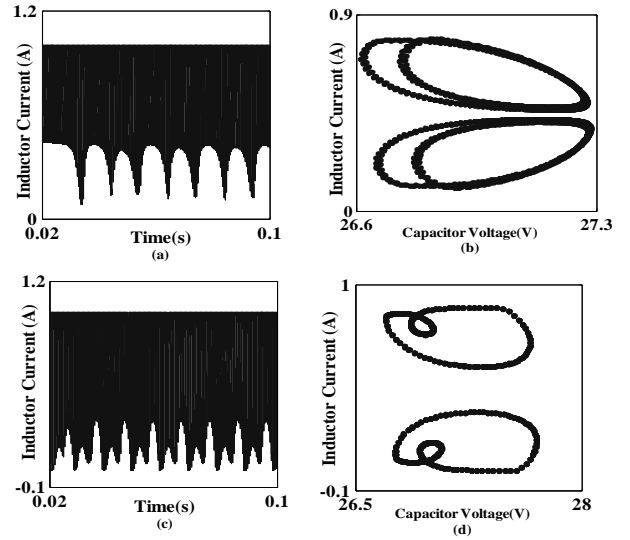


Fig.5. Time response of Inductor current in long span with R (a) $80\ \Omega$ (c) $90\ \Omega$ corresponding Poincare section response in (b) and (d) respectively

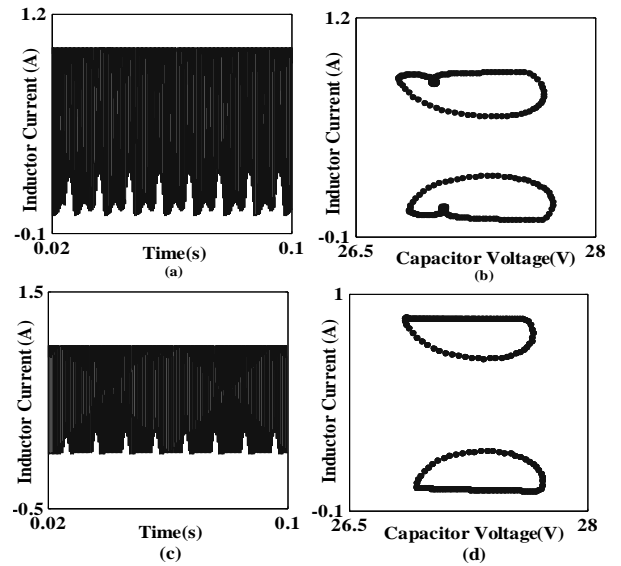


Fig.6. Time plot of Inductor current in long span with R (a) $95\ \Omega$ (c) $100\ \Omega$ corresponding Poincare section response in (b) and (d) respectively

All the above state space structures are having f_s/f_{o2} points, where f_s is switching frequency (25kHz) and f_{o2} is the ripple frequency(100Hz), yielding 250 points for period 1 and for period 2, two identical loops of 125 points each. The frequency spectrum conveys that for period 1 operation, the switching and ripple frequencies are dominating, whereas for period 2 operation, the system is dominated with $(f_{o1}/2)$ Hz and ripple frequency component. Comparing Fig.4 (c) with Fig.6 (c) it is evident that region of stability increases with increase in capacitance value but the system enters into DCM. To consolidate, the bifurcation behavior of rectifier fed boost converter for wide variations in I_{ref} , R and V_{rms} are depicted in Fig.7. It is inferred that system moves from period-1 nature to chaotic mode through border collision. Also, the transitions from period 1 to chaotic mode is not clearly visible.

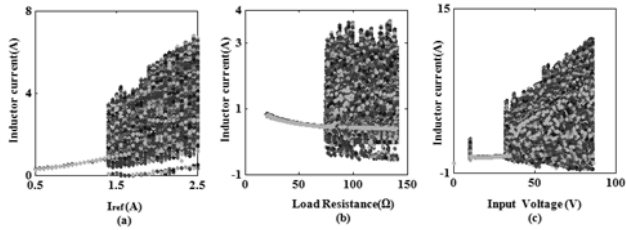


Fig. 7. Bifurcation diagram of peak current mode controlled converter fed from rectifier with bifurcation parameters (a) I_{ref} (b) R (c) V_{rms}

The simulation results are verified using the experimental setup. The hardware implementation of the peak current mode controlled boost converter shown in Fig.1b is made. A 15 V, 50 Hz, single phase ac supply is given to MIC6A4 diode bridge rectifier. The rectified dc is filtered using an electrolytic capacitor of 4700 μ F producing a pulsating dc with the ripple content of 10%, which is fed as an input to the boost converter. The inductor current is sensed using the current sensor LA25A and compared with reference current in LM324 comparator. A clock signal of 25kHz and the comparator output are given as inputs to S and R terminals of SR Flip flop(which is realized using 7402 NOR gate) respectively. The pulse generated is given to the gate of IRF 640 MOSFET switch. The output voltage and inductor current are obtained. The observed period 1, period 2 and chaotic waveforms

of inductor current in long span and short span are shown in Figs. 8(a-d) respectively.

When the results of simulation shown in Fig.3a and experimentation waveform shown in Fig. 8a are compared, they are depicting period 1 behavior for $I_{ref}=1$ A with $R=47 \Omega$ in long span and short span. The hardware result match exactly with the simulation. Similar comparison is made for period 2 operation(Fig.8b with Fig.3c) as well as for chaotic mode period. Experimentation is also carried out for variation in R and C. From the results obtained, it can be concluded that the simulation and experimentation results are showing a very close match.

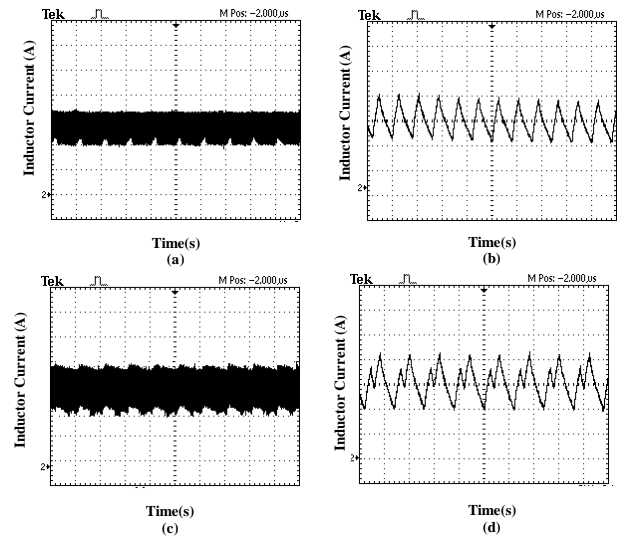


Fig. 8. Time plot of inductor current waveforms. Period 1 operation for $I_{ref}=1$ A (a) in long span (b) in short span ; Period 2 operation for $I_{ref}=1.4$ A (c) in long span (d) in short span [Inductor current is 300 mA/division and Time is 10ms/division]

4. Mathematical analysis

To analyze the stability of power electronic converters, Poincare Map, trajectory sensitivity analysis and Floquet theory are used widely. Fillipov's mathematical approach of stability analysis is widely used in switched mode system [17]-[19] as it locates the eigenvalues and gives the bifurcation point for any piecewise linear smooth system. Fillipov's method uses the switching manifold to calculate the Saltation matrix using which the monodromy matrix is obtained.

The monodromy matrix is given by

$$\Phi_{cycle}(0, T) = S_{i+1} * \Phi_{off}(dT, T) * S_i * \Phi_{on}(0, dT) \quad (5)$$

where ,

S_i is the saltation matrix of i^{th} instant

S_{i+1} is the saltation matrix of $(i+1)^{\text{th}}$ instant

Eigenvalues obtained from monodromy matrix determine the stability of the system (16). For the rectifier fed current mode controlled boost converter the equations represent the vector fields of system before and after switching are as follows.

$$f_- = \begin{bmatrix} \frac{V_{in}}{L} - \frac{x_2}{L} \\ \frac{x_1}{C} - \frac{x_2}{(R*C)} \end{bmatrix} \quad f_+ = \begin{bmatrix} \frac{V_{in}}{L} \\ -\frac{x_2}{(R*C)} \end{bmatrix} \quad (6)$$

$$f_- - f_+ = \begin{bmatrix} -\frac{x_2}{L} \\ +\frac{x_1}{C} \end{bmatrix} \quad (7)$$

Where ,

$$X = [x_1 \quad x_2]^T = [i_L \quad v_o]^T$$

The switching hyper surface is defined as follows

$$h(x, t) = x_1 - I_{ref} \quad (8)$$

The normal to switching hyper surface is

$$n^T = \begin{bmatrix} \frac{\partial h(x, t)}{\partial x_1} & \frac{\partial h(x, t)}{\partial x_2} \end{bmatrix} \quad (9)$$

$$\frac{\partial h(x, t)}{\partial x_1} = 1; \quad \frac{\partial h(x, t)}{\partial x_2} = 0; \quad \frac{\partial h(x, t)}{\partial t} = 0; \quad (10)$$

The following calculations are done to find the saltation matrix

$$(f_- - f_+) * n^T = \begin{bmatrix} -\frac{x_2}{L} \\ +\frac{x_1}{C} \end{bmatrix} [1 \ 0] = \begin{bmatrix} -\frac{x_2}{L} & 0 \\ +\frac{x_1}{C} & 0 \end{bmatrix} \quad (11)$$

$$n^T * f_{on} = [1 \ 0] * \begin{bmatrix} \frac{V_{in}}{L} \\ -\frac{x_2}{(R*C)} \end{bmatrix} \quad (12)$$

$$n^T * f_{on} = \begin{bmatrix} \frac{V_{in}}{L} \end{bmatrix} \quad (13)$$

$$\text{The Saltation matrix, } S = I + \frac{(f_- - f_+) * n^T}{n^T * f_+ + \frac{\partial h}{\partial t}} \quad (14)$$

Where,

$$S_1 = \begin{bmatrix} 1 - \frac{(\frac{x_2}{L})}{h} & 0 \\ \frac{(\frac{x_1}{C})}{h} & 1 \end{bmatrix} \quad S_2 = \begin{bmatrix} 1 & 0 \\ 0 & 1 \end{bmatrix} \quad (15)$$

The monodromy matrix is then calculated using the equation given below.

$$M = S_2 * \exp(A_{off}(1-d)T) * S_1 * \exp(A_{on} * dT) \quad (16)$$

With I_{ref} and R as bifurcation parameters, the floquet multipliers obtained for rectifier fed current mode boost converter are given in Tables I and II and the following conclusions are drawn.

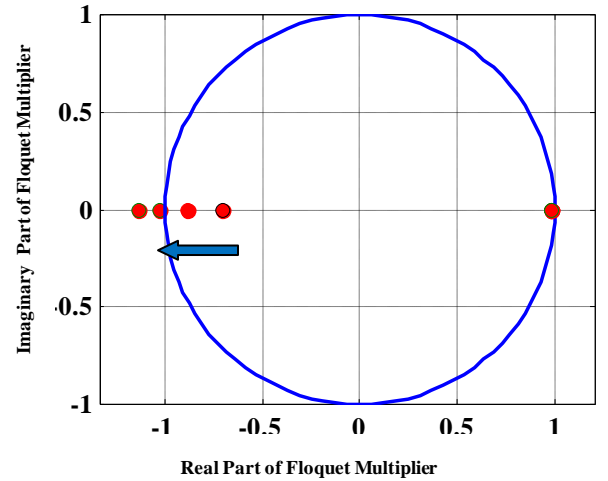


Fig. 9. Movement of eigenvalues in the unit circle with bifurcation parameter as I_{ref}

- When the reference current is chosen as bifurcation parameter
 - For $I_{ref} = 1$ A and 1.2 A, the floquet multipliers are inside the unit circle , indicating stable operation
 - For $I_{ref} = 1.35$ A, the floquet multipliers are just crossing $-1+j0$ revealing unstable operation

- For $I_{ref} = 1.4 \text{ A}$ and 1.5 A , the floquet multipliers are outside the unit circle displaying unstable operation

Table 1 : Floquet multipliers for I_{ref} as bifurcation parameter

I_{ref}	Duty Ratio D	Saltation matrix	Monodromy matrix	Floquet multiplier
1.0	0.4162	$\begin{bmatrix} 1 & 0.2287 \\ 0 & -0.7153 \end{bmatrix}$	$\begin{bmatrix} 0.9755 & 0.4584 \\ 0.0333 & -0.7114 \end{bmatrix}$	0.9845, -0.7204
1.2	0.4711	$\begin{bmatrix} 1 & 0.2859 \\ 0 & -0.8938 \end{bmatrix}$	$\begin{bmatrix} 0.9751 & 0.4934 \\ 0.0377 & -0.8899 \end{bmatrix}$	0.9850, -0.8998
1.35	0.5043	$\begin{bmatrix} 1 & 0.3319 \\ 0 & -1.0210 \end{bmatrix}$	$\begin{bmatrix} 0.9746 & 0.5259 \\ 0.0404 & -1.0170 \end{bmatrix}$	0.9851, -1.0276
1.4	0.5142	$\begin{bmatrix} 1 & 0.3477 \\ 0 & -1.0623 \end{bmatrix}$	$\begin{bmatrix} 0.9739 & 0.5416 \\ 0.0420 & -1.0581 \end{bmatrix}$	0.9852, -1.0691
1.5	0.5324	$\begin{bmatrix} 1 & 0.3798 \\ 0 & -1.1427 \end{bmatrix}$	$\begin{bmatrix} 0.9740 & 0.5624 \\ 0.0426 & -1.1388 \end{bmatrix}$	0.9852, -1.1500

- When load resistance is chosen as bifurcation parameter

-For $R = 47 \Omega$ and 60Ω , the floquet multipliers are inside the unit circle and the system is stable

- For $R = 75 \Omega$, one of the floquet multipliers are about to step outside the unit circle and the system is moving from stable region to unstable region

- For $R \geq 80 \Omega$, one of the floquet multipliers are out of the unit circle and the system is completely unstable. Above conclusions may be depicted in the locus similar to the diagram shown in Fig.9.

Increase in either I_{ref} or R makes the system to lose its periodicity, which is explained above. The comparison made between the simulation, experimentation and analysis shows a very close match.

Table 2 : Floquet multipliers for R as bifurcation parameter

R	Duty Ratio D	Saltation matrix	Monodromy matrix	Floquet Multipliers
47	0.4162	$\begin{bmatrix} 1 & 0.2287 \\ 0 & -0.7153 \end{bmatrix}$	$\begin{bmatrix} 0.9755 & 0.4584 \\ 0.0333 & -0.7114 \end{bmatrix}$	0.9845, -0.7204
60	0.4736	$\begin{bmatrix} 1 & 0.2058 \\ 0 & -0.9020 \end{bmatrix}$	$\begin{bmatrix} 0.9803 & 0.4135 \\ 0.0379 & -0.8980 \end{bmatrix}$	0.9886, -0.9063
75	0.5214	$\begin{bmatrix} 1 & 0.1866 \\ 0 & -1.0917 \end{bmatrix}$	$\begin{bmatrix} 0.9839 & 0.3759 \\ 0.0417 & -1.0877 \end{bmatrix}$	0.9915, -1.0952
80	0.5345	$\begin{bmatrix} 1 & 0.1814 \\ 0 & -1.1540 \end{bmatrix}$	$\begin{bmatrix} 0.9848 & 0.3655 \\ 0.0427 & -1.1464 \end{bmatrix}$	0.9921, -1.1538
100	0.5774	$\begin{bmatrix} 1 & 0.1664 \\ 0 & -1.3684 \end{bmatrix}$	$\begin{bmatrix} 0.9876 & 0.3319 \\ 0.0453 & -1.3645 \end{bmatrix}$	0.9941, -1.3710

5. Interference of sinusoidal signals with different magnitude and frequency

As mentioned earlier in section 3, the rectifier fed boost converter contains two frequency components leading to quasi periodic nature for period 1 operation. The intrusion of spurious signals introduced by PLL, SMPS, PWM generators, etc... will normally be in the form of sinusoidal and triangular signals. These signals get superimposed anywhere and may produce interference in the system. In this section, the presence of sinusoidal interference signal in reference current is analysed for a diode bridge rectifier fed boost converter.

5.1 Sinusoidal interference in reference current with irrational frequency ratio

In this section, the effect of intrusion of unintentional sinusoidal signal in reference current (Fig 1 (a)) with irrational frequency ratio $\alpha_f = f_o/f_s$ [13], where f_o is the frequency of spurious signal, f_s is the switching frequency is analyzed. Since these two frequencies are not proportional to each other, the system tends to oscillate with quasi periodic behavior [20]-[21]. Figs. 10(a) and 10(c) show the quasi periodic behavior of boost converter supplied from a stiff dc source with $\alpha_f = \sqrt{3}/2$ and $\alpha_f = (1+\sqrt{5})/2$ (Golden ratio) respectively. For the same ratios

rectifier fed converter system, introduces a three frequency quasi periodic behavior which are depicted in Figs. 10(b) and 10(d). Similar behavior is also observed for $\alpha_f = (1+\sqrt{2})$ (Silver Ratio).

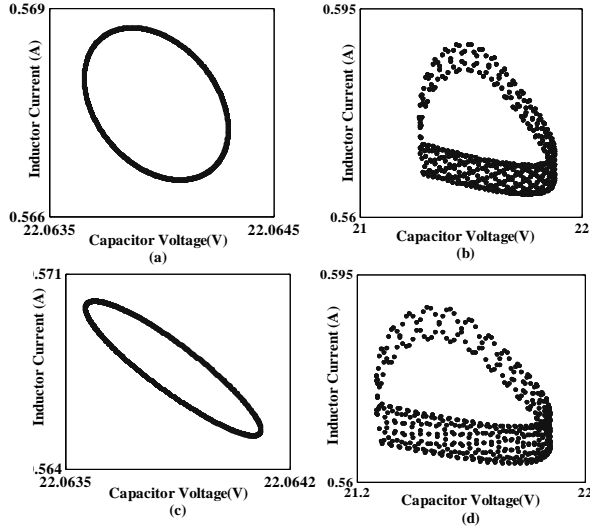


Fig. 10. Sinusoidal interference introduced in reference and its Poincaré sections of responses for $\alpha_v = 0.001$, $\alpha_f = \sqrt{3}/2$ (a) regulated power supply fed boost converter (b) rectifier fed boost converter; for $\alpha_v = 0.001$, $\alpha_f = \text{golden ratio}$ (c) regulated power supply fed boost converter (d) rectifier fed boost converter

5.2 Sinusoidal interference in reference current with rational frequency ratio

The peak current mode controlled boost converter coupled with unintentional intrusion of frequencies having rational frequency ratio [$\alpha_{f1} = f_{01}/f_s = N_{num}/N_{den}$] exhibits a periodic behavior of N_{den} value. For sinusoidal intrusion with a frequency (f_{01}) of 5000 Hz and switching frequency (f_s) of 25000 Hz, the system exhibits a N_{den} period quasi behavior as shown in Fig. 12 (c) with each circle consisting $\alpha_{f2} = f_{01}/f_{02}$ points, where f_{02} is the rectified input frequency 100Hz.

For integer values of the frequency ratio, only one closed path is observed as depicted in Fig. 3(b). For rational frequency ratios of ' $1/n$ ' the system exhibits ' n ' closed curves which are shown in Figs. 11 (a-d).

5.3 Sinusoidal interference in reference current with frequency closer to switching frequency or its rational multiples

When the intruding signal is coupled accidentally, there is a possibility that the intruding frequency is very close to the switching frequency or its rational multiples, the system exhibits intermittent operation. (i.e.) $f_o = kf_s + \hat{f}$ where \hat{f} is a small number compared to f_s and k is a rational number. Considering $\hat{f} = 2$ and $a = 1/2, 1$ the intruding frequencies are 2502 Hz and 5002 Hz.

When ' k ' lies between 0.01 and 0.025 the inductor current is in period 1 with no significant impact of intrusion. For increase in strength of ' k ' to 0.05, the time bifurcation diagram of inductor current displays the intermittent period 2 structure and a fully developed intermittent chaos for 0.075 strength, displayed in Fig. 12 c. Corresponding Poincaré sections are shown in Fig 12 a.

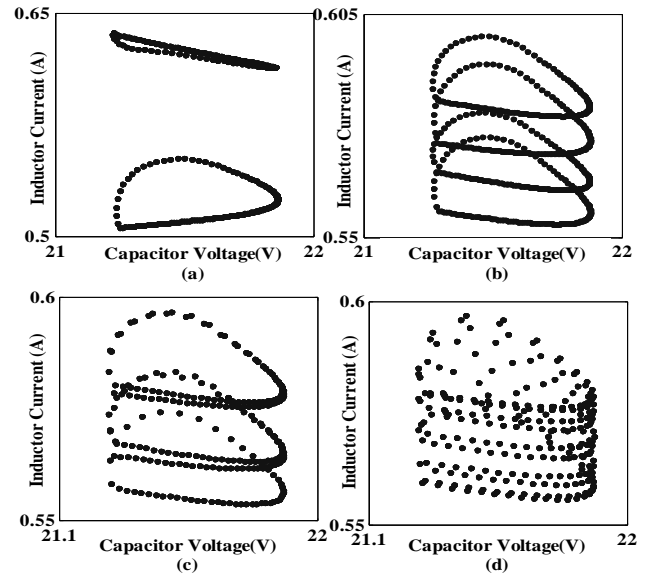


Figure 11. Rectifier fed boost converter with sinusoidal intrusion in reference current having magnitude strength of 0.01 with frequency of intrusion is rational (a) 12500 Hz (b) 6250 Hz (c) 5000 Hz (d) 2500 Hz

Similar phenomenon is observed for the intruding frequency of 12520 Hz shown in Fig. 12 d, corresponding Poincaré sections are shown in Fig 12 b.

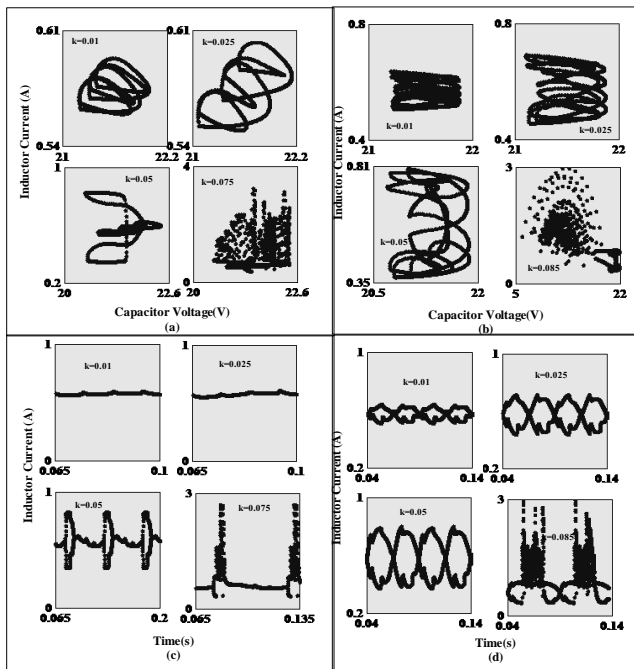


Fig. 12. Poincaré sections of rectifier fed boost converter with sinusoidal intrusion in reference current having intruding frequency of (a) 25020 (b) 12520; Corresponding sampled inductor current waveform with intruding frequency (c) 25020 (d) 12520

The Poincaré sections show mode locked structure for smaller strength of intrusion signals, and the bubbles burst for increase in strength, producing a fully developed chaotic state at the end.

6. Conclusion

The nonlinear dynamics of peak current mode controlled dc dc boost converter fed from a diode bridge rectifier has been studied in this paper. The diode bridge rectifier introduces a 100Hz component along with the switching frequency, making the system to exhibit slow scale and fast scale instabilities, resulting in coexistence. Mathematical analysis is done using Fillipov's method and the Floquet multipliers are calculated from monodromy matrix which supports the simulation and experimental observation. Apart from this, the effect of unintentional intrusions in the reference current has also been studied. The intrusion signal frequency at reference and existing 100 Hz component in the input makes the system to exhibit mode locking behavior.

References:

1. Deane, J. H. B.: *Chaos in a current-mode controlled boost DC-DC converter*. In: IEEE Transactions on Circuits Systems –I (1992), 39, 680–683, 1992.
2. Riku Pollanen: *Simulation of a current-mode controlled DC–DC boost converter in chaotic regime evaluating different simulation methods*. In: Electrical Engineering Springer (2005), pp 35–44, 2005.
3. W.C.Y. Chan, and C.K.Tse: *Study of bifurcation in current-programmed dc/dc boost converters: from quasiperiodicity to period-doubling*. In: IEEE Transactions on Circuits Systems –I (1997), vol. 44, pp. 1129–1142, 1997.
4. Cafagna, D. & Grassi, G.: *Bifurcation analysis and chaotic behaviour in boost converters: Experimental results*. Nonlinear Dynamics (2006), 44, pp 251–262, 2006.
5. S. Parui and S. Banerjee: *Bifurcations due to transition from continuous conduction mode to discontinuous conduction mode in the boost converter*. In: IEEE Transaction on Circuits Systems-I (2003), vol. 50, no. 11, pp. 1464–1469, Nov. 2003.
6. C. K. Tse : *Flip bifurcation and chaos in three-state boost switching regulators*. In: IEEE Transactions Circuits Systems-I (1994), 41, pp. 16–23, Jan. 1994.
7. Biswarup Basak and Sukanya Parui.: *Exploration of Bifurcation and Chaos in Buck Converter Supplied from a Rectifier*. In: IEEE Transaction on Power Electronics. (2010), 25, (6), pp. 1556–1564, 2010.
8. Gerhard F. Bartak Andreas Abart.: *EMI of emissions in the frequency range 2 kHz - 150 kHz* (2013), June 2013.
9. Zhou, Y., Chen, J. N., Iu, H. H. C. & Tse, C. K.: *Complex intermittency in switching converters*. In: International Journal of Bifurcations and Chaos (2008), 18, 121–140, 2008.
10. Wong, S. C., Tse, C. K. & Tam, K. C.: *Intermittent chaotic operation in switching power converters*. In: International Journal of Bifurcations and Chaos, 2004, 14, 2971–2978
11. Ferreira, J. A., Willcock, P. R. & Holm, S. R.: *Sources, paths and traps of conducted EMI in switch mode circuits*. In: Proceedings of IEEE Industry Applications Conference 5–9 Oct 1997 New Orleans, LA, pp. 1584–1591.
12. Tse, C. K., Zhou, Y., Lau, F. C. M. & Qiu, S. S.: *Intermittent chaos in switching power supplies due to*

unintended coupling of spurious signals. In: Proceedings of IEEE Power Electronics Specialist Conference(2003), Acapulco, Mexico, June 15-19, 2003, pp. 642-647.

13. Deivasundari, P., Geetha, R., Uma, G., & Murali, K.: *Chaos, bifurcation and intermittent phenomena in DC-DC converters under resonant parametric perturbation (2013)*. In: European Physics Journal Special Topics 222, 689–697, 2013.

14. Robert, W. Erickson: *Fundamentals of Power Electronics*, Second edition, Springer, Technology and Engineering, Jan 2001.

15. Aroudi, A., Benadero, L., Toribio, E. & Machiche, S.: *Quasiperiodicity and chaos in the DC-DC buck-boost converter*. In: International Journal of Bifurcations and Chaos(2000), **10**, 359-371, 2000.

16. Aroudi, A. & Leyva, R.: *Quasi-periodic route to chaos in a PWM voltage-controlled DC-DC boost converter*. In: IEEE Transactions on Circuits Systems –I (2001), **48**, 967-979, 2001.

17. Damian Giaouris, Abdulmajed Elbkosh, Soumitro Banerjee, Bashar Zahawi, Volker Pickert: *Stability of switching circuits using complete-cycle solution matrices*. In: IEEE International Conference on Industrial Technology (2006) 15-17 Dec. 2006, Mumbai, pp 1954 – 1959.

18. Damian Giaouris, Soumitro Banerjee, Bashar Zahawi, Volker Pickert: *Stability Analysis of the Continuous Conduction Mode Buck Converter via Filippov's Method*. In: IEEE Transactions of Circuits And Systems-I, 2007.

19. P. Deivasundari, G. Uma, K. Kanimozhi.: *Period-bubbling and Mode-locking Instabilities in a Full Bridge DC-AC Buck Inverter*, In: IET Power Electronics(2013), pp1-15, 2013.

20. P. Deivasundari, G. Uma, A. Kavitha.: *Coexistence of Fast-Scale and Slow-Scale Instability in ĆUK Power Factor Correction AC-DC Pre-regulators under Nonlinear Current-Mode Control*(2013). In: IET Power Electronics, 6, No.1, pp 78-87, 2013.

21. Banerjee, S. & Verghese G. C. : *Nonlinear phenomena in power electronics: Attractors, bifurcations, chaos and nonlinear control*(2001), IEEE Press, NY, 2001.